Numerical Investigation of Turbulent Swirling Flows In Flow Metering Configurations

E. von Lavante, J. Yao
University of Duisburg-Essen, Faculty of Engineering
Lotharstr. 1-21, D 47057 Duisburg, Germany
Phone:+49-203-379-3029, FAX: -1304, E-mail:ernst3.vonlavante@uni-due.de

Abstract: Several types of axisymmetric internal configurations were numerically simulated in order to investigate the development of turbulent swirling and non-swirling flows along the axial direction. The governing equations were the Navier-Stokes equations with swirl velocity, requiring the computation of all three velocity components. The turbulence model used in the present work was the quadratic k-ω formulation. Applying the above methods, both swirling and non-swirling flows in a pipe, in a typical Venturi-tube and in an orifice were simulated and the results were analyzed in detail.

Keywords: Swirling flow, Turbulence, Venturi-tube, Swirl decay, Uncertainty

1. Introduction

Precise values of mass flow rates in through-flow configurations are mostly obtained assuming fully developed flow. Any deviations from this flow condition can cause significant errors in the determination of volumetric flow or mass flow. One type of disturbance that is known for its slow decay and for its significant effect on the flow rate measurement is swirl. Swirl may be generated by bends, valves and other devices installed in the pipe system. Since the decay of the swirl is a slow process, the length of the domain influenced by it is quite extensive, about L=100 D, where D is the inner diameter of the pipe.

Many efforts have been undertaken to investigate the influences of the flow swirl on the flow rate measurement. In 1961, Lugt [1] generated swirl by means of a vane and obtained a relation between the non-dimensional swirl parameter and the flow coefficient. A minimum pipe length required to minimize the flow swirl effects upstream of the metering device had been proposed.
In Ferron's work [2] a quantitative relation between the flow velocity profile and the flow coefficient deviation was found. Bluschke et al. [3] implemented a flow straightener between the pipe bend and flow meter in order to effectively reduce the upstream pipe length required for given uncertainty of the flow rate measurement. Akashi et al. [4] presented a new type of perforated plate which was capable to obtain fully developed turbulent flow velocity profile within a short pipe length. Experimental and numerical studies of turbulent swirling pipe flows have been performed by Parchen [5] and Steenbergen et al. [6] resulting in detailed information about the decay rates of swirl in annular pipes. An analytical study of the swirling pipe flow using an approximate form of the turbulent Navier-Stokes equations was carried out by Reader-Harris [7],[8], providing surprisingly realistic description of the swirling flow in pipes.
Most investigations employed flow straighteners or extended upstream length of straight pipe to achieve low levels of disturbance in the metering device. The flow straighteners have, however, several drawbacks such as measurable pressure loss and partially unrealistic flow profiles.

The aim of the work was to investigate the effects of axisymmetric swirling flow on the volumetric flow rate measurement by Venturi tube using numerical simulation. The main purpose was to improve the accuracy of the flow metering. To this end, the present work intended to provide a realistic model of swirling flow by implementing a novel eddy viscosity turbulence model in an axisymmetric computational domain.

2. Numerical Method

In the very beginning of the present work, it was decided not to use one of the major commercial products, as they mostly achieve their robustness at a cost of greatly overpredicted turbulence viscosity. Rather, the authors own simulation program called ACHIEVE, together with newly developed higher order turbulence model, were to be employed.

The non-dimensional Reynolds-averaged Navier-Stokes equations for axisymmetric compressible flow in cylindrical coordinate system x, y, θ can be expressed as:

$$\frac{\partial Q}{\partial t}+\frac{\partial F}{\partial x}+\frac{1}{y}\frac{\partial (yG)}{\partial y}=\frac{1}{y}S_\theta$$

where Q was the vector of conservation flow variables $(\rho, \rho u, \rho v, \rho w, e)^T$. The details of the above equation including the fluxes F and G can be found in, for example, von Lavante and Yao [9]. The gradients in the circumferential direction θ were neglected due to axial symmetry. The components of the usual stress tensor σ_{ij} were given as:

$$\sigma_{ij}=\frac{\mu}{Re_\infty}\left(2S_{ij}-\frac{2}{3}\delta_{ij}\nabla\cdot U\right)-\overline{\rho u_i' u_j'}$$

with the mean strain-rate tensor components S_{ij} for axisymmetric flow

$$S_{xx}=\frac{\partial u}{\partial x},\qquad S_{yy}=\frac{\partial v}{\partial y},\qquad S_{\theta\theta}=\frac{v}{y},$$

$$S_{xy}=\frac{1}{2}(\frac{\partial u}{\partial y}+\frac{\partial v}{\partial x}),\qquad S_{\theta x}=\frac{1}{2}\frac{\partial w}{\partial x},\qquad S_{\theta y}=\frac{1}{2}(\frac{\partial w}{\partial y}-\frac{w}{y})$$

In the above equation, the Reynolds stresses have to be modelled by a proper turbulence model. Many models were available to the authors, but most of them were not capable of correctly predicting the rate of decay of the swirl over long distance of the pipe. The authors decided to implement their version of the quadratic k-ω two-equation model as proposed by Sofialidis et al [10]. The point of departure of this model was the Boussinesque approximation

$$-\overline{\rho u_i' u_j'}=\frac{\mu_t}{Re_\infty}\left(2S_{ij}-\frac{2}{3}\delta_{ij}\nabla\cdot U\right)-\frac{2}{3}\delta_{ij}\rho k$$

The turbulent stress μ_t , defined as $\mu_t \sim \rho k/\omega$, was computed from the strain-rate tensor components S_{ij} using following nonlinear relationship

$$\begin{aligned}-\overline{\rho u_i' u_j'}= &\ \frac{\mu_t}{Re_\infty}\left(2S_{ij}-\tfrac{2}{3}\delta_{ij}\nabla\cdot U\right)-\tfrac{2}{3}\delta_{ij}\rho k\\ &-\frac{\mu_t}{Re_\infty^2}\frac{1}{\omega}\Big[4c_1(S_{ik}S_{kj}-\tfrac{1}{3}S_{kl}S_{kl}\delta_{ij})\\ &+2c_2(\Omega_{ik}S_{kj}+\Omega_{jk}S_{ki})+c_3(\Omega_{ik}\Omega_{kj}-\tfrac{1}{3}\Omega_{lk}\Omega_{lk}\delta_{ij})\Big]\end{aligned}$$

with the rotation Ω_{ij} obtained from

$$\Omega_{xy}=\frac{\partial u}{\partial y}-\frac{\partial v}{\partial x},\qquad \Omega_{\theta x}=\frac{\partial w}{\partial x},\qquad \Omega_{\theta y}=\frac{\partial w}{\partial y}+\frac{w}{y}$$

The details of the model as well as all the modelling parameters and constants are given by Yao [11].

The numerical method for solving the resulting axisymmetric Navier-Stokes equations, coupled with the two turbulence equations, was developed by the authors using modified AUSM-scheme, as introduced by von Lavante and Yao [9]. In this method, the local Riemann-problem is solved using pressure-based flux splitting. The modifications improved the performance of the method for low Mach number flows.

In oder to avoid restrictive stability conditions, appearing in a typical explicit method such as Runge-Kutta time stepping, the governing N-S equations in weak conservative form were solved using an implicit method. The computation was carried out in parallel fashion using a cluster of work stations.

3. Circular Pipe Flow

3.1 Simple Test Case

In order to validate the present numerical method as well as the turbulence model, the simple flow in a circular pipe of diameter D = 0.1 m was simulated for a pipe length L = 150 D. The Reynolds number formed with the pipe diameter $Re_D = \rho u_m D/\mu$ was assumed to be 10^5 , with ρ the density and u_m the bulk velocity.The orthogonal two-dimensional grid consisted of 256 x 64 cells in the axial and radial directions, respectively. The well known velocity profile is shown in Fig. 1 as compared to experimental data obtained by PIV (left). A detailed view of the velocity profile close to the wall as a function of the non-dimensional distance from the wall y^+ can be seen in right part of figure 1.

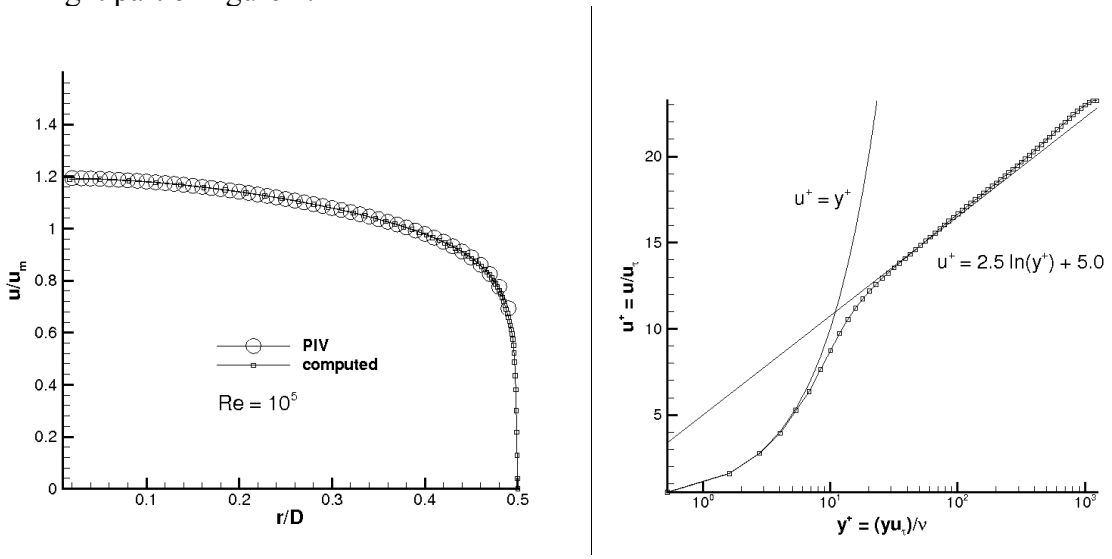

Fig. 1 Comparison of simulated and measured velocity profiles

The agreement between the experimental and theoretical data and the present simulation results is very good.

3.2. Swirling pipe flow

The axisymmetric swirling flow in a straight pipe was simulated using the same strategy as above. All three components of the velocity were solved in the symmetric plane. In terms of the inlet boundary condition, the circumferential velocity was given to initialize the inlet swirl of the flow. For a specified swirl intensity w_m (the mean circumferential velocity), the inlet profile of the cir-

cumferential velocity in the radial direction was obtained using the product of the linear distribution and the turbulent profile. Using this method, the maximum value of w can be determined as $w_{max} = 1.6\ w_m$, appearing at a position of r = 0.12 R away from the wall. On the pipe axis and at the wall, the values of w are zero. All other parameters at the inlet were given according to the fully developed flow profiles in a pipe. Initially, the Reynolds number $Re_D = 10^5$ and the tangential velocity $w_m = 0.5\ u_m$ were assumed. The pipe length was again L = 150 D. The turbulent intensity was assumed constant at the inflow location. The velocity profiles can be viewed in Fig. 2.

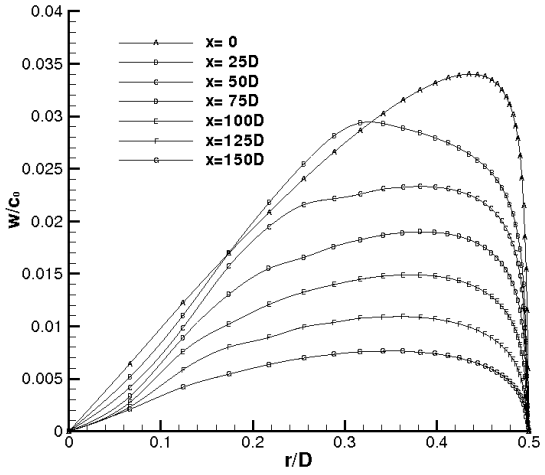

Fig. 2 Velocity profiles at various locations along the pipe axis x.

At x = 25 D, the velocity displays a tendency to move its maximum away from the wall. This is due to the initially assumed constant distribution of the turbulent intensity, as found analytically by Reader-Harris [7]. Further downstream, the correct equilibrium was found as a solution to the governing equation, and the location of the maximum velocity moves to the proper equilibrium position at the wall. The swirl intensity can be expressed by the non-dimensional swirl number

$$S = \frac{2}{R^3 u_m^2} \int_0^R uwr^2 dr$$

The relative swirl number S/S_0 , in which the local swirl number S(x/D) is divided by its initial value at x/D = 0, can be seen in Fig. 3 for different Reynolds numbers for $w_m = 0.5\ u_m$.

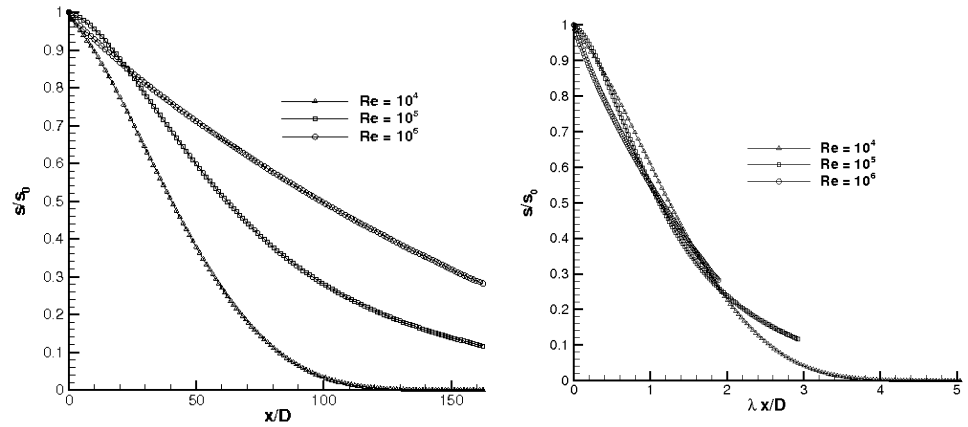

Fig. 3 Decay of the relative Swirl number as function of x/D

The rate of decay is clearly a function of the Reynolds number Re_D and of the non-dimensional distance along the pipe x/D (left). Considering that the friction factor λ is a function of the Reynolds number, a new variable (λ x/D) can be formed that includes the dependency of S on Re. The right diagram in Fig. 3 displays this form of relationship, indicating that the resulting swirl numbers all follow the same curve. Similarly, considering the swirl number for different swirl intensities, the resulting relative swirl number is independent of the swirl intensity, showing the same rate of decay with the axial coordinate x/D.

4. Venturi Tube

The axisymmetric flow in a Venturi tube was simulated numerically using the above described scheme. The inlet diameter of the Venturi tube was denoted D_0 and the diameter of the Venturi throat was selected as $D = 0.7\ D_0$. The convergent and the divergent angles were 21° and 7° , respectively. An orthogonal computational grid with 256 x 64 cells in the axial and radial direction, as shown in Fig. 4, was employed. At the inlet, the axial velocity was set according to the fully developed flow with or without swirl applied previously. The non-reflective boundary conditions was used at the outlet boundary, as described by Yao [11] .

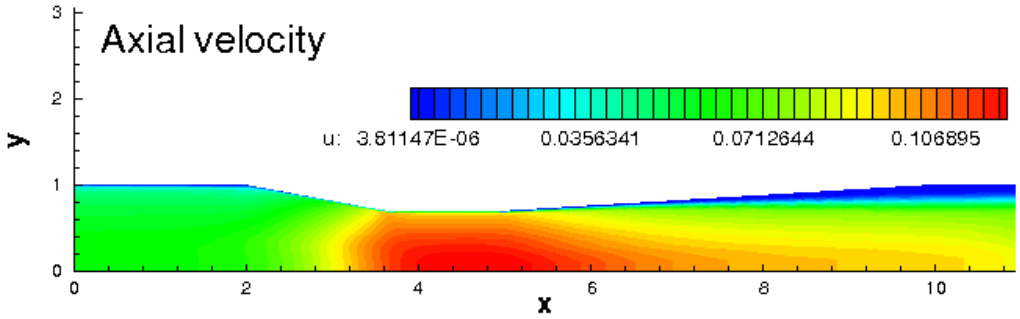

Fig. 4 Shape and velocity distribution in the Venturi tube, $w_m = 0.5\ u_m$

Although the boundary layer thickens in the diffuser, it remains - as predicted - attached. The swirl intensity $w_m = 0$ was assumed initially, making comparison with the DIN standard 1952 [12] with contraction ratio $\beta = 0.7$ possible. As the Reynolds number was varied between 10^5 and 10^6 , the exact value of the inflow diameter could be determined from the corresponding Re_D . The resulting discharge coefficient C_D , compared to the empirical values given in DIN 1952 or, more recently, ISO 5167-4, can be seen in Fig. 5 . The definition of C_D as used presently is

$$C_d' = \frac{Q_m}{A_d\sqrt{2\Delta p\rho}}$$

With Q_m the flow rate, A_d the throat diameter and Δp the pressure differential. For compressible flow, the discharge coefficient has to be corrected by the so called expansion number ε given as

$$\epsilon = \left[\left(\frac{\kappa\tau^{\frac{2}{\kappa}}}{\kappa-1}\right)\left(\frac{1-\beta_d^4}{1-\beta_d^4\tau^{\frac{2}{\kappa}}}\right)\left(\frac{1-\tau^{\frac{\kappa-1}{\kappa}}}{1-\tau}\right)\right]^{0.5}$$

with $\tau = p_2/p_1$. The final form of the discharge coefficient was obtained by $C_d = C'_d/\varepsilon$. The expansion coefficient for different Reynolds numbers and swirl intensities for the case 1 (see below) is given in the right diagram in Fig. 6.

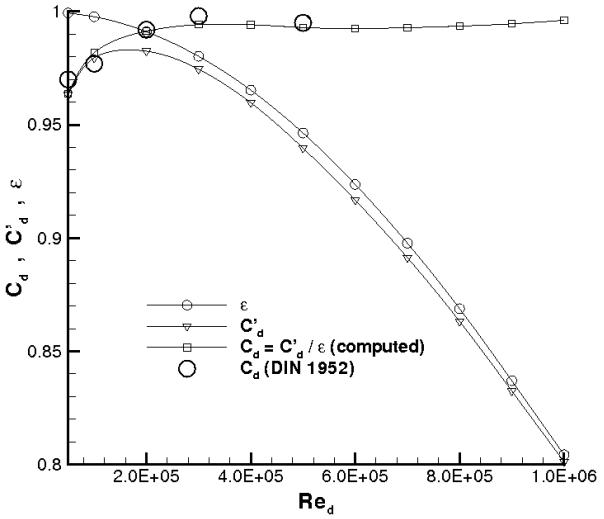

Fig. 5 Discharge coefficient as a function of Re, Venturi tube, $w_m = 0$

After the above validation of the present approach, the flow in the Venturi tube with swirl was finally simulated. Three different swirl (circumferential) velocities were imposed at the inflow:

Case 1: $w^1_m = \pi/2\ w_m \sin(\pi\ r/D)$

Case 2: $w^2_m = 4\ r/D\ w_m\ u(\ r/D)$

Case 3: $w^3_m = \pi/2\ w_m \sin(2\pi\ r/D)$

The corresponding velocity distributions are shown in Fig. 6 for the inflow location x=0 and the throat. The swirl intensities w_m were assumed to be 0.087, 0.173, 0.258, and 0.342.

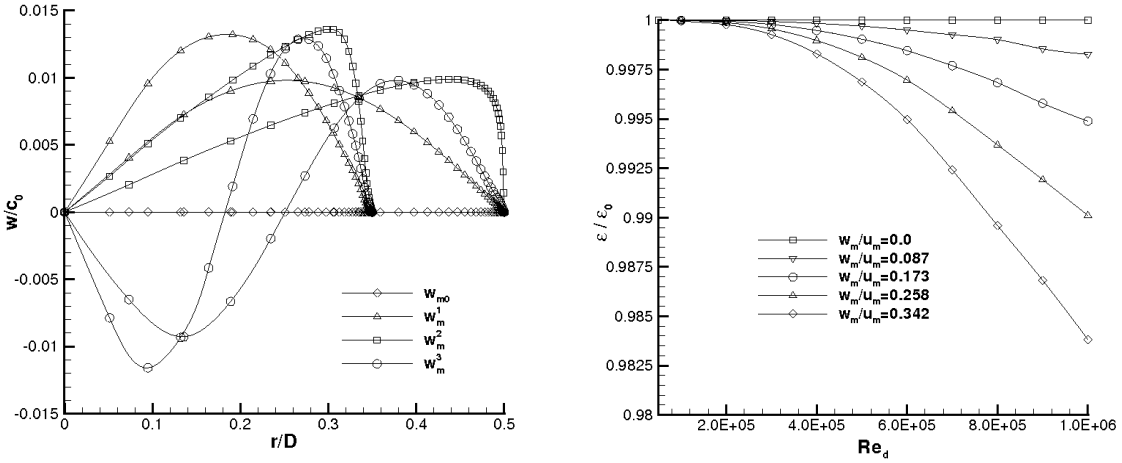

Fig. 6 Circumferential velocity distribution (left), expansion number (right)

The ratio of the discharge coefficients C_D / C_{D0} (C_D with swirl, C_{D0} without swirl) and the flow rate Q_m / Q_{D0} for the cases 1, 2 and 3 are displayed in Figures 7, 8 and 9. Depending on the radial distribution and amplitude of the swirl velocity, the discharge coefficient as well as the indicated

flow rate show significant differences as compared to the case without swirl. The deviation was found to be up to approximately 3 % for case 2 and maximum swirl intensity for the discharge coefficient and over 1% for the flow rate. They both strongly depend on the Reynolds number and the velocity distribution.

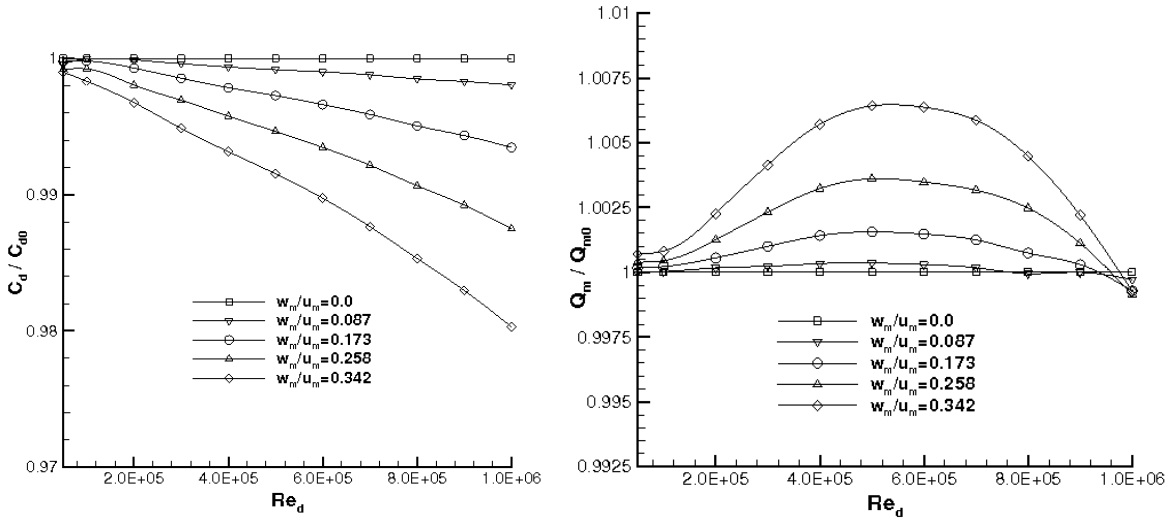

Fig. 7 Discharge coefficient (left) and flow rate (right) for case 1

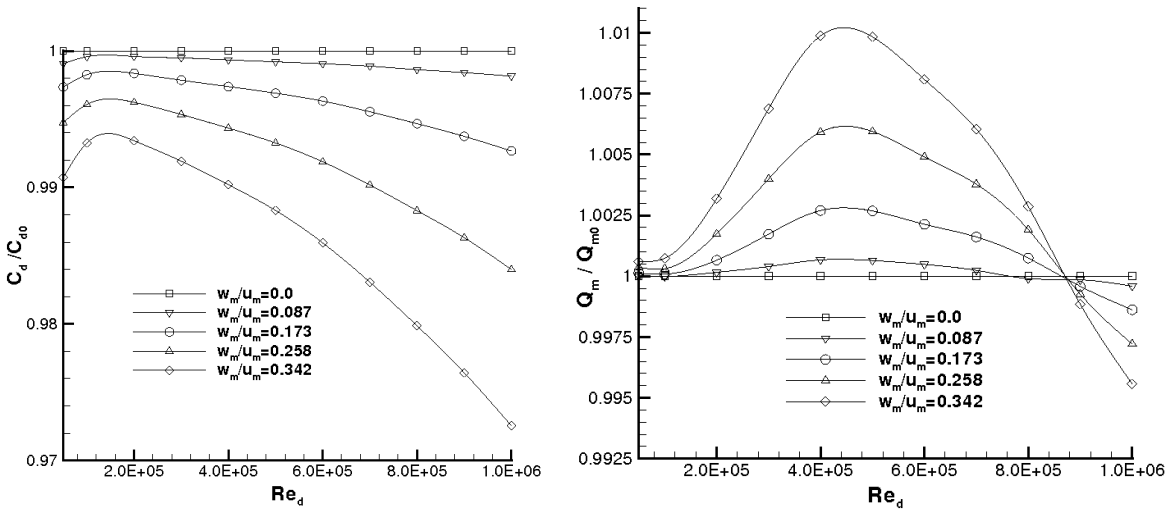

Fig. 8 Discharge coefficient (left) and flow rate (right) for case 2

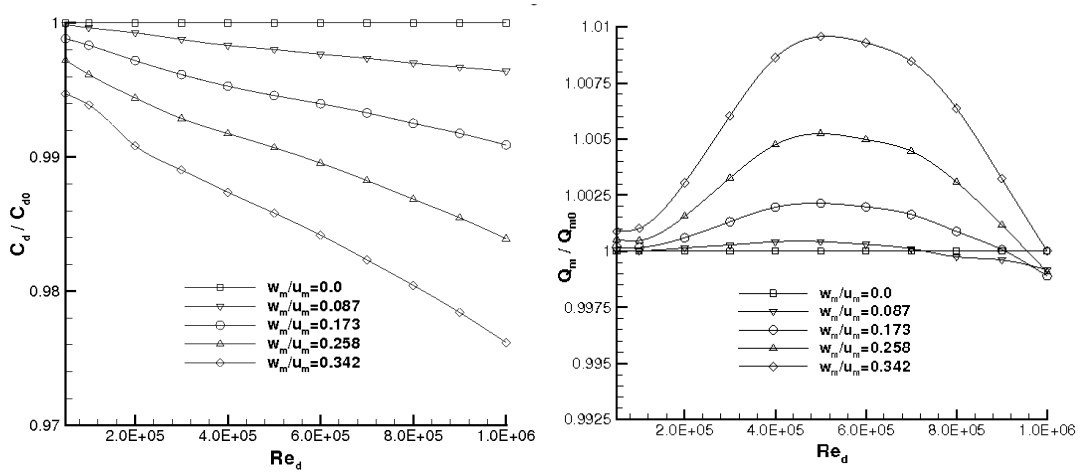

Fig. 9 Discharge coefficient (left) and flow rate (right) for case 3

6. Conclusion

A numerical algorithm for solving the three dimensional axisymmetric internal turbulent flows has been developed. Due to the axial symmetry, the finite difference of the flux vectors in the circumferential direction could be neglected. Much computational time, therefore, was saved and the efficiency of the numerical simulation was significantly increased without negative influences on the simulation accuracy. Both swirling and non-swirling axisymmetric axial flows in a straight pipe were simulated. Very good agreement of the computational and theoretical results of the velocity profiles as well as pressure distributions had been obtained.

The swirl in the flow field in a typical Venturi tube resulted in a deviation of the discharge coefficient and the volumetric flow rates that was significant for flow metering purposes.

The decay of the swirl was comparable to the theoretical and experimental results obtained by other investigators.

Acknowledgment

This work has been supported by a grant from the DFG. The authors are grateful to Prof. Gersten for his comments.

References

[1] Lugt, H., Einfluß der Drallströmung auf die Durchflußzahlen genormter Drosselmeßgeräte', BWK 13 (1961) Nr. 3, March 1961.
[2] Ferron, A.G., Velocity Profile Effects on the Discharge Coefficient of Pressure Differential Meters, Trans. ASME 1962.
[3] Bluschke, H., Hucho, W.H. and Weber, G., Versuche über den Einfluß von Rohrkrümmern auf die Durchflußzahlen von Normventuridüsen und klassischen Venturirohren, Brennst.-Wärme-Kraft 18 (1966) Nr. 2, Februar 1966.
[4] Akashi, K., Watanabe, H. and Koga, K., Flow Rate Measurement in Pipe Line with Many Bends, Technical Review, June 1978.
[5] Parchen, R.R. and Steenbergen, W., An Experimental and Numerical Study of Turbulent Swirling Pipe Flow, Trans. ASME, Vol. 120, March 1998.
[6] Steenbergen, W. and Voskamp, W., The rate of decay of swirl in turbulent pipe flow, Flow Measurement and Instrumentation 9, 1998, pp 67-78.
[7] Reader-Harris, M.J., The decay of swirl in a pipe, Int. J. Heat and Fluid Flow, Vol. 15, No. 3, June 1994.
[8] Reader-Harris, M.J., Brunton, W.C., Sattary, J.A., Installation Effects on Venturi Tubes, ASME Fluid Engineering Division Summer Meeting, FEDSM ’97-3016, 1997.
[9] von Lavante, E. and Yao, J., Simulation of flow in Exhaust Manifold of a Reciprocating Engine, AIAA 93-2954, Orlando, FL, July 1993.
[10] Sofialidis, D and Prinos, P., Wall Suction Effects on the Structure of Fully Developed Turbulent Pipe Flow, J. of Fluid Engineering, Vol. 118, pp33-39, March 1996.
[11] Yao, J., Numerische Simulation der Multi-Dimensionalen Strömung in Kolbenmotoren, Ph.D. Thesis, University of Essen, ISBN 3-8265-3501-4, Shaker Verlag, Aachen, 1998.
[12] DIN 1952 , VDI-Durchflußmeßregeln, Beuth Verlag GmbH, Berlin, 1982.